RSC Advances

REVIEW

View Article Online
View Journal | View Issue

Cite this: *RSC Adv.*, 2022, **12**, 34892

Recent advances in micro-/nanostructure array integrated microfluidic devices for efficient separation of circulating tumor cells

Hanyue Kang,[a] Yuting Xiong,[a] Liang Ma,[b] Tongqing Yang[a] and Xiaobin Xu *[a]

Circulating tumor cells (CTCs) released from the primary tumor to peripheral blood are promising targets for liquid biopsies. Their biological information is vital for early cancer detection, efficacy assessment, and prognostic monitoring. Despite the tremendous clinical applications of CTCs, development of effective separation techniques are still demanding. Traditional separation methods usually use batch processing for enrichment, which inevitably destroy cell integrity and affect the complete information acquisition. Considering the rarity and heterogeneity of CTCs, it is urgent to develop effective separation methods. Microfluidic chips with precise fluid control at the micron level are promising devices for CTC separation. Their further combination with micro-/nanostructure arrays adds more biomolecule binding sites and exhibit unique fluid barrier effect, which significantly improve the CTC capture efficiency, purity, and sensitivity. This review summarized the recent advances in micro-/nanostructure array integrated microfluidic devices for CTC separation, including microrods, nanowires, and 3D micro-/nanostructures. The mechanisms by which these structures contribute to improved capture efficiency are discussed. Two major categories of separation methods, based on the physical and biological properties of CTCs, are discussed separately. Physical separation includes the design and preparation of micro-/nanostructure arrays, while chemical separation additionally involves the selection and modification of specific capture probes. These emerging technologies are expected to become powerful tools for disease diagnosis in the future.

Received 8th October 2022
Accepted 18th November 2022

DOI: 10.1039/d2ra06339e

rsc.li/rsc-advances

1. Introduction

Circulating tumor cells (CTCs), first discovered by Ashworth, are malignant tumor cells shed from solid tumors into circulation.[5] In the peripheral blood, they may be free individual cells or multicell clumps that lodge on distal organs and generate metastatic tumors.[7,8] About 90% of cancer patients die from tumor metastasis, so early diagnosis and treatment are crucial to reducing cancer mortality.[1,10]

In the early stages of tumor growth, CTCs are present in peripheral blood.[11,12] Their concentration is an indicator to evaluate the chemotherapy and patient life expectancy.[13,14] The emerging liquid biopsy is a method for diagnosing and monitoring cancer by detecting CTCs or circulating tumor DNA (ctDNA) in blood. Since CTCs inherit some characteristics from the source tumors, which serve for analyzing their origin, location, and nature.[18,19] Through systematic sample collection, liquid biopsy can get real-time information about primary tissues, which helps to elucidate metastatic cascade mechanisms and select treatment plans.[21–23] The follow-up culture of patients' CTCs also helps personalize anticancer-agent screening. Moreover, the liquid biopsy is facile and non-invasive, prolonging the survival of patients and avoiding the pain from puncture biopsy.[25,26] As a result, CTC detection has great potential for early tumor diagnosis, personalized treatment, and patient prognosis.[29]

In recent years, CTCs have been adjunct to breast cancer screening and prognostic markers for various cancers.[31–33] The primary challenge that hinders the clinical application is the lack of practical technologies to separate the low abundance of CTCs.[34–36] For patients with early-stage cancer, there might be one CTC mixed with five billion red blood cells (RBCs) and ten million white blood cells (WBCs). Second, the similar size and deformability of CTCs and WBCs set obstacles to separation. Third, separation methods are required to handle very small volumes of samples. With advanced knowledge of CTCs, their applications range from simple counting to cell sequencing, which needs to ensure cell integrity. As a result, high-throughput and high-purity methods for enrichment and separation of intact CTC are desperately needed.

Many techniques have been exploited for CTC separation based on physical properties or affinity.[38] Among them, density gradient centrifugation is a simple, rapid, label-free physical

[a]School of Materials Science and Engineering, Tongji University, Shanghai, 201804 China. E-mail: xiaobinxu@tongji.edu.cn
[b]State Key Laboratory of Fluid Power and Mechatronic Systems, Zhejiang University, Hangzhou 310058, China. E-mail: liangma@zju.edu.cn

separation method. Cells in whole blood are divided into several layers based on density differences.[40] The denser WBCs and RBCs precipitate at the bottom of the tube, while CTCs float in the upper layer of the medium. This method retains the viability of CTCs for subsequent culture but tends to leave CTCs in the plasma layer. Filtration is another efficient and straightforward approach regarding cell size.[41,42] Simple and high-throughput filtration of CTCs can be achieved according to their phenotypes. Some small CTCs may be filtered out, while larger WBCs are collected by mistake. Other physical strategies such as electrorotation and dielectrophoresis utilize the differences in surface charge and polarization rate between CTCs and WBCs.[43] They reduce CTC damage to a large extent but require a long sample processing time. Immunoaffinity is an effective and high-purity chemical separation method based on the specific binding of the surface antigens and antibodies.[44] The CellSearch system is the world's first commercially available product approved by U.S. Food and Drug Administration (FDA) for CTC detection and enumeration for malignant disease management. The CTCs in peripheral blood are captured by magnetic nanoparticles bound to specific antibodies. Although non-specific capture of blood cells is avoided, the antigen expression levels vary on the subtypes of tumor cells may cause CTC loss.[45] A summary of the above methods is given in Table 1.

Microfluidic chip often called "lab-on-a-chip," has been used to capture cells or create tumor models due to their advantages, such as high integration, controllable cell manipulation, and convenient viewing.[46–49] Compared to conventional methods, the small injection volumes (10^{-6} to 10^{-12} L) of microfluidic chips reduce sample and reagent consumption.[50] The microchannels' design and the fluid behavior's manipulation allow CTC separation, counting, and release integration on a single chip. The integration avoids loss or contamination from eluting and transferring samples. The surface forces are significantly amplified at the microscale allowing for an effective increase in reaction efficiency, which makes rapid separation and analysis possible. In addition, the portable nature of microfluidic chips has the potential to become point-of-care devices.

Researchers found that microfluidic channels' small surface areas limit their capture capacity. With the development of nanotechnology, the application of micro-/nanostructures to biomedical applications has become a significant trend in today's research. Their small size, high specific surface area, and specially designed structures bring unique physicochemical properties. Compared to flat substrates, the micro-/nanostructure arrays close to cell sizes provide more binding sites, lower cell rolling velocity, and facilitate CTCs-array collision.[63,64] The micro-/nanostructures-embedded microfluidic chip often includes a micro-/nanostructured substrate, a manifold to enclose the chip, and a pump for sample injection. Many structures have been designed, such as microrods, microtubes, nanowires, nanofibers, *etc.* Separation techniques relying on these structures can be mainly classified as physical and chemical. The physical separation method is based on the significant differences in various physical properties (*e.g.*, size, density, and dielectric property) of CTCs and blood cells. In contrast, chemical separation is achieved through various cancer biomarkers on the membranes. Different methods can also be integrated on a single chip for higher performance.

Table 1 Summary of different circulating tumor cells (CTCs) separation methods

Strategy	Approach/substrates	Separation mechanism	Benefits	Limitations	Ref.
Conventional approaches	Density gradient centrifugation	Size density	Simple operation Not limited by surface markers	Large sample volume Blood cell contamination Low sensitivity from CTC loss	51 and 52
	Filtration	Size	Simple operation Not limited by surface markers	WBC contamination Loss of small CTCs CTC deformation	53 and 54
	Electrorotation and dielectrophoresis	Dielectric property	Label-free High purity and viability	Low efficiency	55 and 56
	Immunocapture	Affinity	High specificity, purity and sensitivity	High cost Limited antibody availability Complicated process	57 and 58
Microfluidic with micro-/nanostructure (physical approach)	Microrods	Size	Label-free Low cost	Complicated nanofabrication	1 and 4
	DLD		Simple operation	Low specificity and purity	15 and 59
	3D micro-/nanostructures	Adhesion	High throughput		30
Microfluidic with micro-/nanostructure (chemical approach)	DLD-patterned microrods	Size affinity	High capture efficiency, specificity and purity	High cost	37 and 39
	Microrods	Affinity		Limited antibody availability	20, 28, 60 and 61
	Nanowires				3, 9, 17, 27 and 62
	3D micro-/nanostructures			Complicated nanofabrication and modification	2, 6, 16 and 24

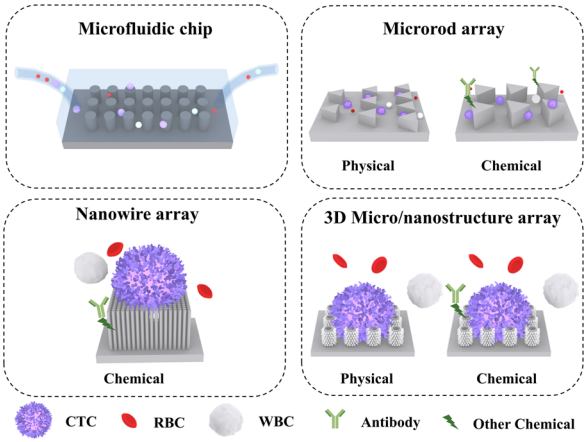

Fig. 1 Schematic illustrations of (A) micro-/nanostructure integrated microfluidic device for CTC capture. (B) 1D microrod arrays. (C) 1D nanowire array. (D) 3D hierarchical micro-/nanostructure arrays.

While there have been many reviews on separation CTCs by microfluidic chips, most focus on presenting the differences between physical and chemical separation methods, with little discussion on the role of micro-/nanostructures in improving separation efficiency. With the continuous development of micro and nano fabrication and its deeper integration into the biomedical field, understanding the mechanisms by which different micro and nanostructures promote improved capture efficiency is essential.

This article focuses on the recent advances in micro-/nanostructure integrated microfluidic chips for CTC separation. Three micro-/nanostructures are introduced, including microrods, nanowires, and 3D micro-/nanostructures (Fig. 1). On this basis, physical and chemical separation methods are discussed in subsequent sections. The classic and innovative literature summarized in this review will shed light on improving the efficiency of CTC separation.

2. Microrod array integrated microfluidic devices

Microrods are one-dimensional (1D) microstructures with a length-to-diameter aspect ratio of 3–5. They are typically fabricated through photolithography and soft lithography on either rigid materials (such as Si,[65,66] glass,[67] PMMA[68,69]) or soft materials (such as polydimethylsiloxane, PDMS[70,71]). The number and topology of microrods can be designed to realize label-free separation based on biophysical properties or specific capture with modified chemical markers.[72] When combined with microfluidic devices, the physical interaction of fluid dynamics with the micro-/nanostructure can improve CTC sorting efficiency.[73] In the following, we discussed the two major types of CTC separating mechanisms based on microrods, one is physical, and the other is chemical.

2.1 CTC physical separation by microrod arrays

Some representative physical separation methods achieved remarkable results, such as membrane or microstructure filtration, hydrodynamic separation (*e.g.*, deterministic lateral displacement and inertial focus), and dielectrophoresis. The physical separation methods are low-cost techniques that rely solely on the structure without biochemical modifications. They preserve the integrity and viability of CTCs, which helps genetic technology obtain accurate cancer information. However, WBCs close in size to CTCs may become interfering factors. This section mainly focuses on microrod arrays for filtration and deterministic lateral displacement.

2.1.1 Filtration. Filtration is a common method to realize mixture separation based on deformability and size. The reported size of most CTCs is 14–26 μm, while WBCs are 8–20 μm and RBCs are only 7–8.5 μm.[74] Therefore, the sizes and gaps of microrods can be adjusted to retain large CTCs between the gaps and filter small blood cells. The tumor cells show a greater nuclear-cytoplasmic ratio than WBCs.[75] Since the nucleoplasm is more rigid and viscous than the cytoplasm, WBCs have stronger deformability.[76] They can be easily washed away even if they are accidentally stuck between the gaps.

As shown in Fig. 2A, Park *et al.* developed a matrix of tapered constrictions based on differences in cellular deformability.[1] The funnel opening size gradually decreases from the bottom entrance row of 18 μm to the top exit row of 2 μm. The funnel opening size gradually decreases from the bottom entrance row to the top exit row. With the blood sample continuous oscillatory flow through this array, each cell is deformed through a funnel-shaped contraction. When reaching the row of 6 μm constrictions, small RBCs or easily deformed WBCs cross the funnel constriction. At the same time, CTCs are constrained between two rows and wait to be collected by a constant rightward flow. The separation efficiency of the device remains relatively stable at 93–96%. Since oscillatory flow avoids the clogging of high cell density samples, the pre-treatment dilution of the sample is omitted.

In addition to the separation according to cell deformability, Lu *et al.* proposed a size-based device combining a streamline-based focus-separation deceleration design with a triangular prism array (Fig. 2B).[4] As the blood flows through the seven focus-separation apparatuses, CTCs are continuously pushed into the main channel. In contrast, some blood cells are removed through the branch channel. This design concentrates CTCs and reduces contamination of blood cells. Subsequently, the fluid flows into the capture apparatus with triangular barrier layer structures of decreasing gaps (14, 12, 10, 8 μm). Different sizes of CTCs were trapped while the remaining blood cells flowed through.

The microrod filtration is a label-free platform that overcomes dependence on specific capture probes. Without complicated modification operations, this method is simple, low cost, and maintains the integrity of CTCs for downstream analysis. However, clogging is inevitable when processing samples with high cell density. In addition, the flow rate must be carefully controlled to avoid cell damage.

2.1.2 Deterministic lateral displacement. Compared with size-based filtration, deterministic lateral displacement (DLD) avoids the clogging risk. The DLD microrod array was first reported by Huang *et al.* to separate bacterial artificial

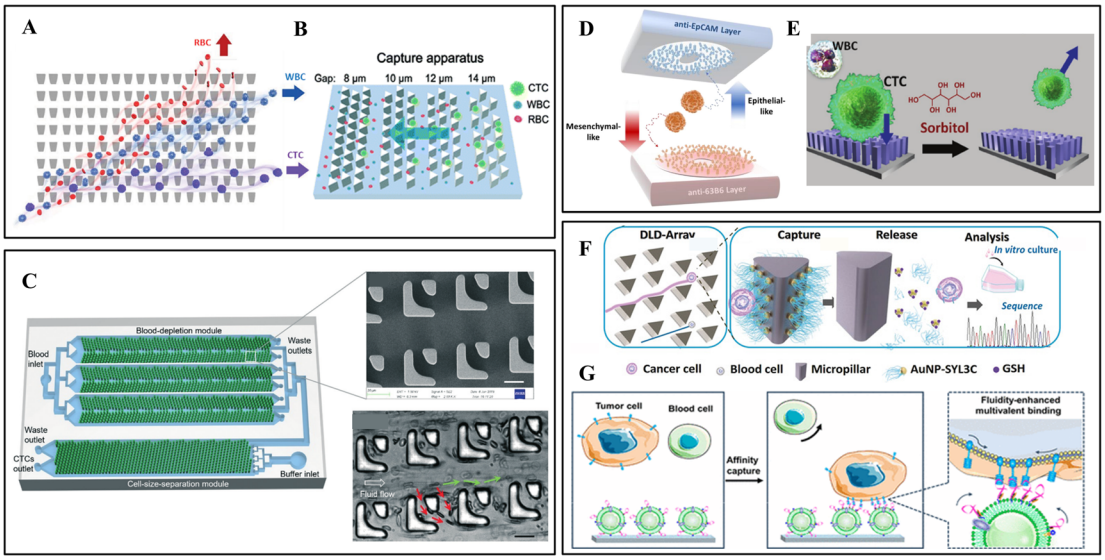

Fig. 2 Microrod array integrated microfluidic devices. (A) CTCs filter through a matrix of funnel constrictions. Reprinted with permission from ref. 1. Copyright (2016) John Wiley and Sons. (B) Streamline focus enrichment and triangular prism array for CTC filtration. Reprinted with permission from ref. 4. Copyright (2020) Royal Society of Chemistry. (C) Cascaded filter DLD microchip for size-based CTC separation. Scale bar, 20 μm. Reprinted with permission from ref. 15. Copyright (2020) Royal Society of Chemistry. (D) Dual-immunopatterned (DIP) device modified by anti-EpCAM and anti-63B6. Reprinted with permission from ref. 20. Copyright (2018) Elsevier. (E) CTC capture on poly(3,4-ethylene-dioxythiophene) s (PEDOT) rods array and release by competition with sorbitol. Reprinted with permission from ref. 28. Copyright (2018) John Wiley and Sons. (F) DLD-patterned triangular micropillars modified with multivalent aptamer-functionalized nanospheres for CTC capture and release. Reprinted with permission from ref. 37. Copyright (2019) John Wiley and Sons. (G) DLD-patterned triangular micropillars decorated with aptamer-functionalized leukocyte membrane nanovesicles. Reprinted with permission from ref. 39. Copyright (2020) American Chemical Society.

chromosomes.[77] The separation mechanism that controls the trajectory of cells was elucidated by fluorescent polystyrene microspheres. Each row of the microrods laterally shifts at a critical distance from the previous row. The critical cutoff diameters (D_c) can be determined by optimizing the gap distance and microrod size. Because of the fluid drag force, cells smaller than D_c flow in the same stream (zigzag mode), while the larger ones are deflected into the adjacent stream by additional force from microrods (bumping mode).

Based on this theory, Loutherback *et al.* designed a triangular-microrod DLD array for continuous-flow capture of CTCs.[59] They increased the gap of microrods to 42 μm, corresponding to a D_c of 7 μm, and changed the shape to a triangle, which provides greater throughput and reduces the possibility of clogging. For viscous blood samples, 85% of CTCs were successfully separated at a flow rate of 10 mL min^{-1}. Later, Liu *et al.* designed a high-throughput cascaded filter-DLD chip, as illustrated in Fig. 2C.[15] The filter unit contains two spaced micro-posts. When the sample flows through the filter-DLD array, smaller blood cells are partially removed or move in zigzag mode (red arrows), while CTCs and WBCs move in bumping mode (green arrows). In this chip, the filter-DLD arrays were integrated into two modules. Three sets of symmetric arrays in the blood-depletion module enrich CTCs and a portion of WBCs. Then, large CTCs were collected in the cell-size-separation module with increasing D_c from 8 μm to 22 μm. Compared with conventional DLD structures, filter-DLD shows smaller D_c and a higher depletion rate of smaller cells.

The deterministic lateral displacement also shows the advantages of simple operation, low cost, and minor damage to CTCs. Nevertheless, there are some disadvantages to overcome. The complex blood environment makes cellular interactions challenging to control, and the efficiency will be reduced with high cell concentration.

2.2 CTC separation by chemical modified microrod arrays

In comparison, chemical-based separation relies on binding specific capture probes and cancer biomarkers, which are molecular changes measured between normal and cancerous tissues. The most widely used method immobilizes specific capture probes inside the microchannels. When the sample is injected into the chip, CTCs will be captured while the remaining blood cells flow out. To extend capture capacity, microrod arrays on flat substrates provide larger binding sites and facilitate cell–surface interactions.

2.2.1 Antibody modification. The prevailing method is to modify the structural surface with antibodies corresponding to the specific antigen expressed by CTC. Epithelial cell adhesion molecule (EpCAM), a transmembrane glycoprotein frequently overexpressed in epithelial origin solid cancers but absent from blood cells, has been a marker for CTC identification.[36,78] However, the EpCAM-only based method may limit the detection of CTCs from other types of cancer. Hence, there are also tissue-specific membrane antigens aimed at specific tumor cells with higher purity, such as prostate-specific membrane antigen (PSMA) in prostate carcinoma.[79] In addition to the positive

selection, there is also a negative selection towards WBCs with their unique CD45 and CD66b markers. The RBCs are first removed through Ficoll gradient centrifugation or chemical lysis. Then, large amounts of WBCs are depleted, and the uncaptured CTCs will be collected. This method reduces CTC loss at the expense of purity. Positive selection can also be added subsequently to achieve high capture efficiency and purity.

In 2007, Nagrath *et al.* prepared an antibody-coated microposts platform to efficiently and selectively isolate CTCs from peripheral blood.[60] After modifying anti-EpCAM, this chip identified CTCs for metastatic lung, prostate, pancreatic, breast, and colon cancers with a 99% success rate. Conventional silicon microrod arrays have poor optical transparency and require complex processing. For these reasons, Yan *et al.* prepared a PDMS microrod array device with high optical transparency using soft lithography and rapid prototyping.[61] This device shows high capture efficiency for different cancer cells and allows direct monitoring of the captured cells under the microscope.

However, CTCs may undergo epithelial–mesenchymal transition (EMT), which downregulates the EpCAM expression and leads to false-negative results. Therefore, some researchers explored antibody cocktails to capture the missed CTCs. As shown in Fig. 2D, Kang *et al.* designed a dual-immunopatterned (DIP) device composed of aligned two layers with rings of polar arrayed microrods.[20] The rings are alternately formed from the two layers and maintain the same spacing. The upper and bottom layers were modified with anti-EpCAM for epithelial CTCs and newly developed anti-63B6 for mesenchymal CTCs. The difference in the antigens expressed on the CTC surface can be indicated by comparing their numbers on the two layers. This device achieved good results in separating heterogeneous subtype of CTCs in blood.

Antibody capture avoids non-specific adsorption of blood cells, achieving high efficiency and purity. The release usually requires hydrolytic digestion of the antigen on the cell membrane, hindering subsequent molecular characteristics analysis.[80] Shen *et al.* proposed a method for gentle release of CTC based on competitive binding to other reagents.[28] They prepared a phenylboronic acid (PBA)-grafted nanoimprinted poly(3,4-ethylene-dioxythiophene)s (PEDOT) rods array and modified anti-EpCAM *via* PBA–oligosaccharide bonding (Fig. 2E). The captured CTCs can be released by exposure to sorbitol, which has a stronger affinity to PBA. Through this process, CTCs from blood were substantially purified with well-preserved RNA.

2.2.2 Aptamer modification. Aptamers are also known as chemical antibodies. They are synthetic single stranded DNA/RNA sequences obtained through systematic evolution of ligands by exponential enrichment (SELEX), binding to molecules, cells, *etc.*[81,82] By suitable screening from the abundant and diverse aptamers, CTC subpopulations can be captured efficiently. Most importantly, the captured CTC can be nondestructively released through various methods, such as nuclease digestion and complementary strand hybridization.[83,84] Therefore, they have been considered ideal recognition ligands for CTC capture and release.[23]

Song *et al.* from Chaoyong Yang's group developed a multivalent aptamer-modified micropillar array (Fig. 2F).[37] Under the principle of DLD, each row of the micropillars has a fixed shift, CTCs larger than the D_c of 13 μm will have constant cell–pillar collisions, while smaller blood cells will migrate in the direction of flow. The triangular micropillars create a smooth hydrodynamic force gradient to slow the flow velocity and achieve maximum CTC attachment. Gold nanoparticles modified on micropillars contain aptamers that bind to cell membranes. The captured CTCs were released nondestructively through the thiol exchange reaction at the AuNP–aptamer interface. However, the non-specifically captured blood cells remained on the surface, which improved the purity. Later, this group modified aptamer-functionalized leukocyte membrane nanovesicles on the triangular micropillars (Fig. 2G).[39] Nanovesicles were obtained through disruption and extrusion of biotinylated WBCs and inherited the nature of surface membranes. The blood cell resistance of the membrane reduces the background cells, and the membrane fluidity allows lateral rearrangement of aptamers to achieve high-affinity binding. Moreover, the captured CTCs show excellent CTC viability (97.6%) due to the cushioning of the soft membranes.

Although the aptamers demonstrated excellent capture and release capabilities, they were not as widely used as expected. The primary reason is that their performance is affected by the complex blood environment. In whole blood, they may be rapidly degraded by nucleases or influenced by high-abundance blood cells and proteins.[85,86] Therefore, it is necessary to synthesize aptamers that remain effective in the complex blood environment.

3. Nanowire integrated microfluidic devices

Nanostructures in the tissue microenvironment have a significant role in modulating cellular behavior and biochemical support. Nanowires are one-dimensional (1D) microstructures with a high length-to-diameter aspect ratio, usually greater than 1000. Nanowires embedded in substrates precisely mimic the characteristics of cellular microstructures such as extracellular matrix, which in turn are used for cellular behavior studies in biomedical applications. Their diameters are close to the sizes of cellular pseudopods, greatly enhancing cell–substrate adhesion.[87–89] By precisely controlling the length, density and arrangement of nanowires, multiple feature size structural substrates can be designed to explore the relationship with CTC capture efficiency.

The nanowires are usually obtained by photolithography combined with wet etching techniques, hydrothermal growth, chemical vapor deposition, *etc.* These techniques are now relatively mature and easy to operate. A typical nanowire microfluidic device for CTC capture is the "NanoVelcro chip" cell affinity substrate concept pioneered by Tseng Lab at UCLA.[90] This chip can achieve dynamic and efficient CTC

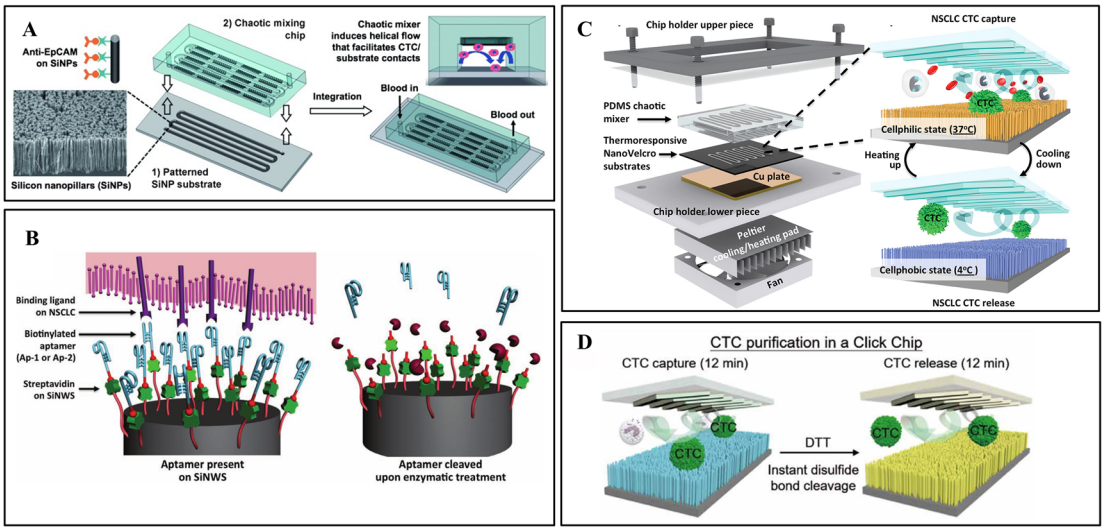

Fig. 3 Nanowire integrated microfluidic devices. (A) Antibody modified silicon nanowires with chaotic mixer for immunoaffinity capture. Reprinted with permission from ref. 3. Copyright (2011) John Wiley and Sons. (B) CTC capture and release from aptamer-coated SiNWs. Reprinted with permission from ref. 9. Copyright (2013) John Wiley and Sons. (C) Digitally programmed thermoresponsive NanoVelcro CTC purification system for precisely temperature-dependent capture and release. Reprinted with permission from ref. 17. Copyright (2014) American Chemical Society. (D) The disulfide cleavage-driven release on covalent chemistry-based silicon nanowires. Reprinted with permission from ref. 27. Copyright (2019) American Association for the Advancement of Science.

capture by constructing a trapping agent-coated nanostructured substrate. In addition to the common SiNWs, the concept of "NanoVelcro" has been applied to other nanosubstrates, such as conjugated polymer nanofeatures and nanofibers.[91,92]

The NanoVelcro chip developed by this team has undergone three generations of innovation for different clinical applications. The first generation NanoVelcro chip comprises a patterned SiNW substrate and an overlaid PDMS chaotic mixer, as shown in Fig. 3A.[3] The innovative chaotic mixer induced the vertical flow of the sample to enhance CTC–SiNWS contact frequency. The optimized condition achieved more than 85% capture rate in artificial samples. This device was further applied to CTC collection and enumeration to monitor the treatment of cancer patients.[93]

While NanoVelcro chips allow for efficient and reproducible CTC counting in a clinical setting, empowering NanoVelcro chips with cellular release remains challenging. A diagnostic assay platform capable of efficient capture and specific release of CTCs will pave the way for subsequent downstream applications such as molecular characterization and functional analysis. For release purposes, they introduced an improved first-generation NanoVelcro chip that replaces the antibody-based capture agent (*i.e.*, anti-EpCAM) with two DNA aptamers, Ap-1 and Ap-2 (Fig. 3B).[9] Genetically engineered endonucleases were used to specifically degrade the SiNW-grafted DNA aptamers, enabling CTC capture followed by release. Another group proposed a sandwich structured peptide–silicon nanowire (Pe–SiNWS)-based microfluidic device which first employs enzymatic release to collect CTC from blood samples.[62] Pe–SiNWS facilitated specific capture, biorelease, and accurate analysis of CTC. This technology can achieve 95.6% CTC capture. After enzymatic digestion, good CTC purity of 28.5% and cell viability of 93.5% can be obtained.

To simplify the procedure and improve cell viability for clinical application, a digitally programmed thermoresponsive-NanoVelcro chip was developed.[17] Thermally responsive polymer brushes, covalently-linked biotin group, and antibodies were modified on SiNWs.[94] The thermosensitive nanonylon matrix can capture and release CTCs at 37 °C and 4 °C, respectively (Fig. 3C). The release is through internalizing antibodies from the conformational changes in the backbones of polymer brushes. The integrated thermal-electric Peltier cooling/heating system with a thermocouple sensor enables device temperature control. Gentle operating parameters minimize CTC viability and molecular integrity disruption by applying physiologically durable stimuli.

Recently, studies have shown that click chemistry can yield highly pure biomolecules.[94] Based on the above research, Tseng lab developed a covalent chemistry-based capture/release platform ("Click Chip").[27] A pair of highly reactive click chemistry motifs (Tz and TCO) were modified on SiNWs and CTCs, leading to instant, high-purity, and irreversible CTC captures under mild conditions. Subsequently, a disulfide cleavage agent was utilized to release CTCs without non-specifically captured WBCs (Fig. 3D). The better-preserved CTC mRNA has been applied to downstream studies for evaluating treatment and monitoring disease progression.

4. 3D micro-/nanostructure array integrated microfluidic devices

Nanostructures are known to provide high specific surface area, thus allowing more immunoaffinity molecules to be immobilized on the surface. With the continuous development of nanotechnology and bionanotechnology, new innovative

structures were introduced to improve the performance of biochips. Nowadays, three-dimensional hierarchical nanostructures with optimized performance are a hot topic of current research in enhancing biological cell capture. The 3D micro-/nanostructure here refers to the composition of basic structural units from 1D micro-/nanostructure. For higher capture efficiency, nanowires (*e.g.*, TiO_2, ZnO, ITO) are often combined with microrods to form hierarchical topography.[90,95] The longitudinally and horizontally combined multi-dimensional forms of micro–nano structures can be generated through various techniques, such as photolithography, atomic layer deposition, multi-step chemical vapor deposition, hydrothermal growth or other combinatorial techniques.[96,97] In addition, some researchers have been inspired by nature to prepare 3D micro-/nanostructures using natural structures such as gecko feet, rose petals, and butterfly wings, achieving good results.[98,99]

Recent studies have shown that hierarchical nanostructured substrates exhibit further improved cell capture efficiency and device sensitivity compared to one-dimensional vertical micro–nanostructures (*e.g.*, nanopillars, nanowires) and one-dimensional horizontal nanostructured (*e.g.*, nanofibers) substrates.[97] Firstly, the hierarchical nanostructures are better matched in size to the cellular filamentous pseudopods. Secondly, the horizontal branching of the structure can further enhance the interaction between the cellular filamentous pseudopods and the material, improving the contact with the fluid. Besides, the longitudinal structural branches act in concert to further rivet cells, providing additional physical binding sites for cell capture.

For instance, Qiu *et al.* proposed a 3D micro-/nanostructure from hydrothermally growing TiO_2 nanorods on the sidewall of hexagonally patterned silicon microrods (Fig. 4A).[2] After antibody modification, this device showed almost twice the capture efficiency of the pure Si nanorods at a range of cell densities. The highest capture efficiency of 76.7% ± 7.1% can be achieved for the artificial whole blood sample. In addition, the excellent biocompatibility of TiO_2 nanorods enables the captured CTCs to grow and proliferate well in the microchannel, offering a possible approach for cancer diagnosis and personalized treatment aimed at patients with very low CTC abundance.

In another study, Hui *et al.* prepared a self-sterilizing and reproducible ZnO-coated PDMS micrometer column array for home testing.[6] Antibody mixture (anti-EpCAM and anti-vimentin) was engrafted to the structural surface to provide more accurate results. The ZnO nanograss enhances the interaction with cells and reduces the adhesion of WBCs. Moreover, ZnO shows robust antibacterial ability making sterile environments unnecessary. Ultimately, the captured CTCs could be released by dissolving a thin layer of ZnO in an acidic solution. As shown in Fig. 4B, the remaining seed layer can be used for the second preparation of ZnO coating. Cui *et al.* followed the same principle to prepare a ZnO-coated PDMS gear structure array.[100] Besides high surface area, the gear structure provides a suitable location for CTC attachment. Due to the increased roughness of the ZnO coating, fully extended pseudopodia have been observed under high magnification SEM images. The captured CTC can also be released by dissolving ZnO in a mild acidic solution, ensuring high viability.

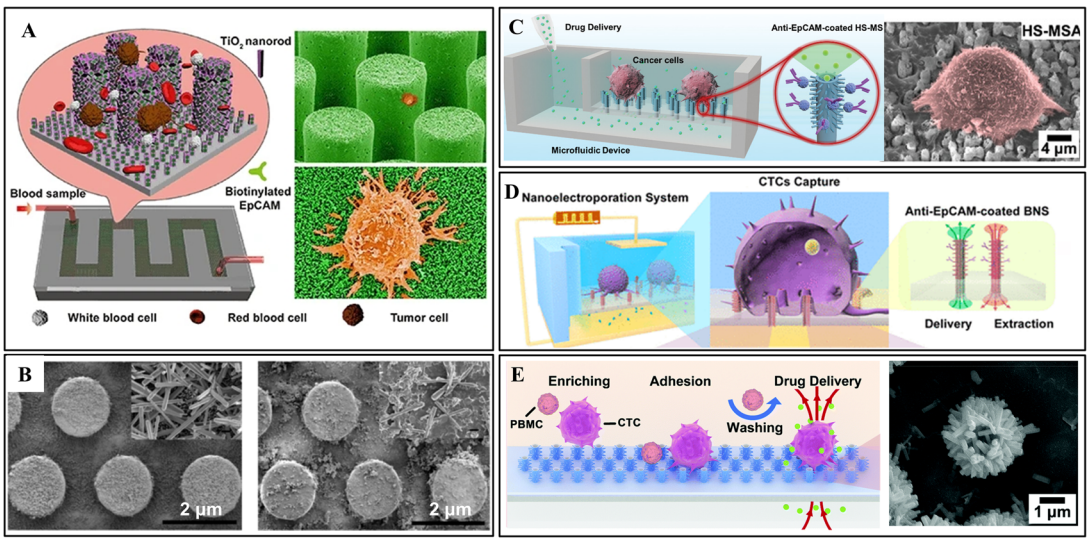

Fig. 4 3D micro-/nanostructure integrated microfluidic devices. (A) Vertical growth of TiO_2 nanorods on silicon nanopillars for immunoaffinity capture. Reprinted with permission from ref. 2. Copyright (2017) Springer Nature. (B) ZnO coated PDMS microrod array from the first synthesis cycle (left) and the second cycle (right). Reprinted with permission from ref. 6. Copyright (2018) American Chemical Society. (C) Hierarchical spiky microstraw array-integrated microfluidic device for immunoaffinity capture and *in situ* chemical manipulation. Reprinted with permission from ref. 16. Copyright (2019) John Wiley and Sons. (D) Branched nanostraw-electroporation platform for immunoaffinity capture, downstream regulation and monitoring intracellular activities. Reprinted with permission from ref. 24. Copyright (2019) American Chemical Society. (E) Hybrid TiO_2/ZnO branched microtube array for antibody-free separation and *in situ* regulation. Reprinted with permission from ref. 30. Copyright (2020) Royal Society of Chemistry.

Table 2 Typical micro-/nanostructure array integrated microfluidic devices for CTC capture

Structure	Modification	CTC source	Sample	Volume	Flow rate or time	Capture efficiency	Ref.
Microrod	None	UM-UC13	Human blood	5 mL	1 mL h^{-1}	>90%	1
		HeLa, MCF-7	Rabbit blood	2 mL	40 mL h^{-1}	95.8% ± 0.9%	4
		MDA-MB-231				95.7% ± 3.5%	
						96.3% ± 1.2%	
		NCI-H226				91.3% ± 3.2%	
		MCF10A	Human blood	5 mL	10 mL min^{-1}	>85%	59
		A549, K562	Human blood	10 mL	60 mL h^{-1}	>96%	15
	Anti-EpCAM	NCI-H1650	Human blood	n/a	1 mL h^{-1}	65%	60
		MCF-7	PBS buffer	1 mL	1 mL h^{-1}	~88%	61
		NCI-H1650	Human blood				
	Anti-EpCAM	MCF-7	PBS buffer	1 mL	1 mL h^{-1}	93.81% ± 8.58%	20
	Anti-63B6	MDA-MB-231	Human blood			95.13% ± 4.28%	
	Anti-EpCAM	LNCap, PC3	Human blood	100 μL	60 min	72.5% ± 3.0%	28
		22Rv1				75.2% ± 3.2%	
						67.8% ± 1.7%	
	SYL3C aptamer	SW480	PBS buffer	n/a	1 mL h^{-1}	86.7–89.4%	37
		LNCap, K-562					
		KATO IIIl	Human blood				
		SW480, MCF-7	DMEM		0.35 mL h^{-1}	84.3–91.3%	39
		HCT 116	Human blood				
		LNCap					
Nanowire	Anti-EpCAM	MCF-7	DMEM	n/a	1 mL h^{-1}	>95%	3
		PC3, T24	Human blood				
	Ap1, Ap2 aptamer	A549, HCC827	PBS buffer	1 mL	1 mL h^{-1}	>85%	9
			Human blood				
	Peptides CKAAKN	BxPC3	Artificial sample	200 μL	1 mL h^{-1}	95.6%	62
	Anti-EpCAM	H1957, H2228	Artificial sample	n/a	0.5 mL h^{-1}	90–95%	17
		A549	Human blood				
		HCC78, H2228	Human blood	200 μL	1 mL h^{-1}	94 ± 3%	27
		HCC827					
		H1985					
3D hybrid micro-/nanostructure	Anti-EpCAM	MCF-7	Human blood	1 mL	0.5 mL h^{-1}	76.7 ± 7.1%	2
	Anti-EpCAM	MCF-7	PBS buffer	1 mL	30 min	85.47 ± 1.88%	6
			Artificial blood				
	Anti-vimentin	MDA-MB231	Human blood				
	Anti-EpCAM	MCF-7	Human blood	200 μL	60 min	84 ± 6.2%	16
						85 ± 2.5%	
		PC3		400 μL	60 min	93.1 ± 5.1%	24
						86.0 ± 9.5%	
	None	MCF-7	Artificial sample	1 mL	6 h	~93.1%	30
		HeLa				~79.6%	
		PC3				~79.2%	

In recent years, cell *in situ* chemical manipulations has become the exploration target. Nicholas A. Melosh's group at Stanford University demonstrated alumina-coated polycarbonate nanostraws to deliver small molecules and ions into the cytosol.[101] To avoid perforating cell membranes, they developed nondestructive electroporation delivery by opening transient pores during perforation and resealing the membrane after voltage removal.[102] Subsequently, the nanostraws have been proven effective in delivering signaling ions and extracting proteins and mRNA.[103,104]

Inspired by their studies, Xi Xie's group fabricated a hierarchical spiky microstraw array (HS-MSA) for high-efficient CTC capture and drug delivery (Fig. 4C).[16] The ZnO nanospikes were hydrothermally grown on polycarbonate microstraws. Then, an alumina layer was deposited on the surface to avoid potential cytotoxicity. After anti-EpCAM modification, high capture efficiency (≈84%) was achieved due to the closer contact interfaces provided by nanospikes. The hollow microstraws deliver drugs to local cells through the microfluidic channels, enabling release-free *in situ* cancer cell drug screening. Following this study, electroporation was also applied to allow intracellular drug delivery and content extraction (Fig. 4D).[24]

To break through the limitation of antibodies, they explored a hybrid TiO_2/ZnO branched microtube array (HBMTA) for antibody-free capture of adherent tumor cells (Fig. 4E).[30] After 6 h of incubation, cancer cells preferentially adhered to HBMTA due to the landing sites provided by the rough surface. In contrast, the blood cells freely floated in the sample and were washed off through fluidic shear.

5. Summary and prospect

CTCs have high clinical value as disease markers in cancer diversity research, diagnosis, treatment, and monitoring. In this review, we have summarized the representative works on the micro-/nanostructures array (microrods, nanowires, and 3D hybrid micro-/nanostructures) integrated microfluidic devices for CTC capture during recent years. The large surface area and fluidic perturbation phenomenon of these structures significantly improve CTC capture and screening. The captured CTCs have been applied to explore cancer mechanisms and solve complex biological problems. In recent years, microrod array integrated microfluidic devices using physical and chemical separation methods have enabled small-scale clinical applications. The most common application is CTC enumeration for helping diagnose, detecting cancer progression, and predicting poor prognosis.[105–109] The genetic analysis of the captured CTCs provides effective treatment options.[110] Besides, CTCs have also been applied to assess sensitivity to chemotherapeutic agents, which helps in the selection of appropriate drugs.[111] However, the blockage generated by the physical separation, the loss by low-expression antigens in chemical separation, and the effects of stress forces on CTCs due to fluid perturbation make the large-scale clinical application of these techniques still challenging. In downstream applications, it is also critical to achieving controllable CTC release or single-site individual CTC release to investigate the heterogeneity without cell damage. Also, improve specific selectivity (*e.g.*, missed detection due to low expression in mesenchymal cells) for genomic or protein profiling.[112] In addition, a large number of clinical samples are required to ensure the feasibility, reproducibility, and sensitivity of microfluidics before it is introduced into clinical CTC analysis practice. Recently, researchers have strived for 3D micro-/nanostructures by hydrothermal growing or etching nanowires on the surface of microrods, which show better capture performance and high detection repeatability. The innovative bio-inspired 3D structures also open up avenues for CTC capture. The benefits and limitations of micro-/nanostructures mentioned in this paper are summarized in Table 1, and each device is shown in Table 2. In the last few years, 3D printing has emerged for fabricating truly 3D microfluidic devices in one step at a low cost.[113,114] With technological change, microfluidic devices will move toward miniaturization and integration, eventually realizing integrated clinical applications for CTC enrichment, separation, and detection, such as single-cell sequencing, metabolic analysis, and drug sensitivity. Portable, miniaturized, and rapid clinical diagnosis and treatment of cancer may emerge in the future.

Author contributions

All authors have read and agreed to the published version of the manuscript. HYK and YTX were involved in writing (original draft, and review and editing); LM and TQY were involved in supervision; XBX was involved in supervision and writing (review and editing and visualization).

Conflicts of interest

The authors declare no conflict of interest.

Acknowledgements

This work is financially support by the National Natural Science Foundation of China (Grant No. 51901159), and the Fundamental Research Funds for the Central Universities.

References

1 E. S. Park, C. Jin, Q. Guo, R. R. Ang, S. P. Duffy, K. Matthews, A. Azad, H. Abdi, T. Todenhofer, J. Bazov, K. N. Chi, P. C. Black and H. S. Ma, *Small*, 2016, **12**, 1909–1919.
2 J. C. Qiu, K. Zhao, L. L. Li, X. Yu, W. B. Guo, S. Wang, X. D. Zhang, C. F. Pan, Z. L. Wang and H. Liu, *Nano Res.*, 2017, **10**, 776–784.
3 S. T. Wang, K. Liu, J. A. Liu, Z. T. F. Yu, X. W. Xu, L. B. Zhao, T. Lee, E. K. Lee, J. Reiss, Y. K. Lee, L. W. K. Chung, J. T. Huang, M. Rettig, D. Seligson, K. N. Duraiswamy, C. K. F. Shen and H. R. Tseng, *Angew. Chem., Int. Ed.*, 2011, **50**, 3084–3088.
4 C. Y. Lu, J. Xu, J. T. Han, X. Li, N. T. Xue, J. S. Li, W. H. Wu, X. L. Sun, Y. G. Wang, Q. Ouyang, G. Yang and C. X. Luo, *Lab Chip*, 2020, **20**, 4094–4105.
5 Z. Y. Shen, A. G. Wu and X. Y. Chen, *Chem. Soc. Rev.*, 2017, **46**, 2038–2056.
6 L. L. Hui, Y. Su, T. T. Ye, Z. Liu, Q. C. Tian, C. J. He, Y. Q. Zhao, P. Chen, X. J. Wang, W. D. Hang, Y. Luo and B. Wang, *ACS Appl. Mater. Interfaces*, 2018, **10**, 207–218.
7 D. X. Nguyen, P. D. Bos and J. Massague, *Nat. Rev. Cancer*, 2009, **9**, 274–284.
8 A. Gribko, J. Kunzel, D. Wunsch, Q. Lu, S. M. Nagel, S. K. Knauer, R. H. Stauber and G. B. Ding, *Int. J. Nanomed.*, 2019, **14**, 4187–4209.
9 Q. L. Shen, L. Xu, L. B. Zhao, D. X. Wu, Y. S. Fan, Y. L. Zhou, W. H. OuYang, X. C. Xu, Z. Zhang, M. Song, T. Lee, M. A. Garcia, B. Xiong, S. Hou, H. R. Tseng and X. H. Fang, *Adv. Mater.*, 2013, **25**, 2368–2373.
10 A. W. Lambert, D. R. Pattabiraman and R. A. Weinberg, *Cell*, 2017, **168**, 670–691.
11 J. M. Lloyd, C. M. McIver, S. A. Stephenson, P. J. Hewett, N. Rieger and J. E. Hardingham, *Clin. Cancer Res.*, 2006, **12**, 417–423.
12 C. A. Klein, *Nat. Rev. Cancer*, 2009, **9**, 302–312.
13 H. I. Scher, X. Y. Jia, J. S. de Bono, M. Fleisher, K. J. Pienta, D. Raghavan and G. Heller, *Lancet Oncol.*, 2009, **10**, 233–239.
14 X. T. Li, B. B. Chen, M. He, H. Wang, G. Y. Xiao, B. Yang and B. Hu, *Biosens. Bioelectron.*, 2017, **90**, 343–348.
15 Z. B. Liu, Y. Q. Huang, W. L. Liang, J. Bai, H. T. Feng, Z. H. Fang, G. Tian, Y. J. Zhu, H. B. Zhang, Y. X. Wang, A. X. Liu and Y. Chen, *Lab Chip*, 2021, **21**, 2881–2891.
16 G. He, C. D. Yang, J. M. Feng, J. M. Wu, L. F. Zhou, R. Wen, S. Huang, Q. N. Wu, F. M. Liu, H. J. Chen, T. Hang and X. Xie, *Adv. Funct. Mater.*, 2019, **29**, 1806484.

17 Z. F. Ke, M. Lin, J. F. Chen, J. S. Choi, Y. Zhang, A. Fong, A. J. Liang, S. F. Chen, Q. Y. Li, W. F. Fang, P. S. Zhang, M. A. Garcia, T. Lee, M. Song, H. A. Lin, H. C. Zhao, S. C. Luo, S. Hou, H. H. Yu and H. R. Tseng, *ACS Nano*, 2015, **9**, 62–70.
18 G. P. Gupta and J. Massague, *Cell*, 2006, **127**, 679–695.
19 P. S. Steeg, *Nat. Med.*, 2006, **12**, 895–904.
20 Y. T. Kang, Y. J. Kim, J. Bu, S. Chen, Y. H. Cho, H. M. Lee, C. J. Ryu, Y. Lim and S. W. Han, *Sens. Actuators, B*, 2018, **260**, 320–330.
21 J. W. Franses, J. Philipp, P. Missios, I. Bhan, A. Liu, C. Yashaswini, E. Tai, H. L. Zhu, M. Ligorio, B. Nicholson, E. M. Tassoni, N. Desai, A. S. Kulkarni, A. Szabolcs, T. S. Hong, A. S. Liss, C. Fernandez-del Castillo, D. P. Ryan, S. Maheswaran, D. A. Haber, G. Q. Daley and D. T. Ting, *Nat. Commun.*, 2020, **11**, 3303.
22 R. Klotz, A. Thomas, T. Teng, S. M. Han, O. Iriondo, L. Li, S. Restrepo-Vassalli, A. Wang, N. Izadian, M. MacKay, B. S. Moon, K. J. Liu, S. K. Ganesan, G. Lee, D. S. Kang, C. S. Walmsley, C. Pinto, M. F. Press, W. Lu, J. Lu, D. Juric, A. Bardia, J. Hicks, B. Salhia, F. Attenello, A. D. Smith and M. Yu, *Cancer Discovery*, 2020, **10**, 86–103.
23 L. L. Wu, L. Zhu, M. J. Huang, J. Song, H. M. Zhang, Y. L. Song, W. Wang and C. Y. Yang, *Trends Anal. Chem.*, 2019, **117**, 69–77.
24 G. He, J. M. Feng, A. H. Zhang, L. F. Zhou, R. Wen, J. M. Wu, C. D. Yang, J. Yang, C. W. Li, D. M. Chen, J. Wang, N. Hu and X. Xie, *Nano Lett.*, 2019, **19**, 7201–7209.
25 R. Vaidyanathan, R. H. Soon, P. Zhang, K. Jiang and C. T. Lim, *Lab Chip*, 2019, **19**, 11–34.
26 J. Sierra, J. Marrugo-Ramirez, R. Rodriguez-Trujillo, M. Mir and J. Samitier, *Sensors*, 2020, **20**, 1317.
27 J. T. Dong, Y. J. Jan, J. Cheng, R. Y. Zhang, M. Meng, M. Smalley, P. J. Chen, X. H. Tang, P. Tseng, L. R. Bao, T. Y. Huang, D. J. Zhou, Y. P. Liu, X. S. Chai, H. Zhang, A. Q. Zhou, V. G. Agopian, E. M. Posadas, J. J. Shyue, S. J. Jonas, P. S. Weiss, M. Y. Li, G. J. Zheng, H. H. Yu, M. P. Zhao, H. R. Tseng and Y. Z. Zhu, *Sci. Adv.*, 2019, **5**, eva9186.
28 M. Y. Shen, J. F. Chen, C. H. Luo, S. Lee, C. H. Li, Y. L. Yang, Y. H. Tsai, B. C. Ho, L. R. Bao, T. J. Lee, Y. J. Jan, Y. Z. Zhu, S. Cheng, F. Y. Feng, P. L. Chen, S. Hou, V. Agopian, Y. S. Hsiao, H. R. Tseng, E. M. Posadas and H. H. Yu, *Adv. Healthcare Mater.*, 2018, **7**, 1700701.
29 J. S. de Bono, H. I. Scher, R. B. Montgomery, C. Parker, M. C. Miller, H. Tissing, G. V. Doyle, L. Terstappen, K. J. Pienta and D. Raghavan, *Clin. Cancer Res.*, 2008, **14**, 6302–6309.
30 J. M. Feng, J. S. Mo, A. H. Zhang, D. Liu, L. F. Zhou, T. Hang, C. Yang, Q. N. Wu, D. H. Xia, R. Wen, J. Yang, Y. P. Feng, Y. Huang, N. Hu, G. He and X. Xie, *Nanoscale*, 2020, **12**, 5103–5113.
31 Y. Gao, W. H. Fan, C. H. Duan, W. H. Zhao, J. Zhang and X. X. Kang, *Front. Oncol.*, 2021, **11**, 643003.
32 A. Matikas, A. Kotsakis, S. Apostolaki, H. Politaki, M. Perraki, K. Kalbakis, M. Nikolaou, P. Economopoulou, D. Hatzidaki and V. Georgoulias, *Br. J. Cancer*, 2022, **11**, 1563–1569.
33 H. I. Scher, A. J. Armstrong, J. D. Schonhoft, A. Gill, J. L. Zhao, E. Barnett, E. Carbone, J. Lu, E. S. Antonarakis, J. Luo, S. Tagawa, C. H. dos Anjos, Q. Yang, D. George, R. Szmulewitz, D. C. Danila, R. Wenstrup, M. Gonen and S. Halabi, *Eur. J. Cancer*, 2021, **150**, 83–94.
34 M. Antfolk, C. Magnusson, P. Augustsson, H. Lija and T. Laurell, *Anal. Chem.*, 2015, **87**, 9322–9328.
35 F. Del Ben, M. Turetta, G. Celetti, A. Piruska, M. Bulfoni, D. Cesselli, W. T. S. Huck and G. Scoles, *Angew. Chem., Int. Ed.*, 2016, **55**, 8581–8584.
36 H. M. Pei, L. Li, Z. J. Han, Y. G. Wang and B. Tang, *Lab Chip*, 2020, **20**, 3854–3875.
37 Y. L. Song, Y. Z. Shi, M. J. Huang, W. Wang, Y. Wang, J. Cheng, Z. C. Lei, Z. Zhu and C. Y. Yang, *Angew. Chem., Int. Ed.*, 2019, **58**, 2236–2240.
38 J. Kaiser, *Science*, 2010, **327**, 1072–1074.
39 L. L. Wu, H. M. Ding, X. Qu, X. N. Shi, J. M. Yang, M. J. Huang, J. L. Zhang, H. M. Zhang, J. Song, L. Zhu, Y. L. Song, Y. Q. Ma and C. Y. Yang, *J. Am. Chem. Soc.*, 2020, **142**, 4800–4806.
40 P. Banko, S. Y. Lee, V. Nagygyorgy, M. Zrinyi, C. H. Chae, D. H. Cho and A. Telekes, *J. Hematol. Oncol.*, 2019, **12**, 48.
41 Y. T. Kang, I. Doh, J. Byun, H. J. Chang and Y. H. Cho, *Theranostics*, 2017, **7**, 3179–3191.
42 S. J. Hao, Y. Wan, Y. Q. Xia, X. Zou and S. Y. Zheng, *Adv. Drug Delivery Rev.*, 2018, **125**, 3–20.
43 F. F. Becker, X. B. Wang, Y. Huang, R. Pethig, J. Vykoukal and P. R. C. Gascoyne, *Proc. Natl. Acad. Sci. U. S. A.*, 1995, **92**, 860–864.
44 V. Murlidhar, L. Rivera-Baez and S. Nagrath, *Small*, 2016, **12**, 4450–4463.
45 M. Jamal-Hanjani, E. Thanopoulou, K. S. Peggs, S. A. Quezada and C. Swanton, *Curr. Opin. Pharmacol.*, 2013, **13**, 497–503.
46 A. Dalili, E. Samiei and M. Hoorfar, *Analyst*, 2019, **144**, 87–113.
47 T. A. Duncombe, A. M. Tentori and A. E. Herr, *Nat. Rev. Mol. Cell Biol.*, 2015, **16**, 554–567.
48 X. Mu, W. F. Zheng, J. S. Sun, W. Zhang and X. Y. Jiang, *Small*, 2013, **9**, 9–21.
49 M. Li, X. E. Song, S. Jin and K. M. Ye, *Bio-Des. Manuf.*, 2021, **4**, 526–540.
50 H. Okano, T. Konishi, T. Suzuki, T. Suzuki, S. Ariyasu, S. Aoki, R. Abe and M. Hayase, *Biomed. Microdevices*, 2015, **17**, 59.
51 A. G. Oh, D. W. Lee and Y. H. Cho, *Sens. Actuators, B*, 2012, **166**, 24–30.
52 J. M. Park, J. Y. Lee, J. G. Lee, H. Jeong, J. M. Oh, Y. J. Kim, D. Park, M. S. Kim, H. J. Lee, J. H. Oh, S. S. Lee, W. Y. Lee and N. Huh, *Anal. Chem.*, 2012, **84**, 7400–7407.
53 Y. C. Ma, L. Wang and F. L. Yu, *Technol. Cancer Res. Treat.*, 2013, **12**, 295–309.
54 D. L. Adams, P. X. Zhu, O. V. Makarova, S. S. Martin, M. Charpentier, S. Chumsri, S. H. Li, P. Amstutz and C. M. Tang, *RSC Adv.*, 2014, **4**, 4334–4342.

55 P. R. C. Gascoyne, J. Noshari, T. J. Anderson and F. F. Becker, *Electrophoresis*, 2009, **30**, 1388–1398.
56 V. Gupta, I. Jafferji, M. Garza, V. O. Melnikova, D. K. Hasegawa, R. Pethig and D. W. Davis, *Biomicrofluidics*, 2012, **6**, 024133.
57 A. L. Allan, S. A. Vantyghem, A. B. Tuck, A. F. Chambers, I. H. Chin-Yee and M. Keeney, *Cytometry, Part A*, 2005, **65A**, 4–14.
58 A. H. Talasaz, A. A. Powell, D. E. Huber, J. G. Berbee, K. H. Roh, W. Yu, W. Z. Xiao, M. M. Davis, R. F. Pease, M. N. Mindrinos, S. S. Jeffrey and R. W. Davis, *Proc. Natl. Acad. Sci. U. S. A.*, 2009, **106**, 3970–3975.
59 K. Loutherback, J. D'Silva, L. Y. Liu, A. Wu, R. H. Austin and J. C. Sturm, *AIP Adv.*, 2012, **2**, 042107.
60 S. Nagrath, L. V. Sequist, S. Maheswaran, D. W. Bell, D. Irimia, L. Ulkus, M. R. Smith, E. L. Kwak, S. Digumarthy, A. Muzikansky, P. Ryan, U. J. Balis, R. G. Tompkins, D. A. Haber and M. Toner, *Nature*, 2007, **450**, 1235–1239.
61 S. Q. Yan, X. Zhang, X. F. Dai, X. J. Feng, W. Du and B. F. Liu, *ACS Appl. Mater. Interfaces*, 2016, **8**, 33457–33463.
62 Q. L. Shen, H. T. Yang, C. X. Peng, H. Zhu, J. Mei, S. Huang, B. Chen, J. Liu, W. B. Wu and S. K. Cao, *Int. J. Nanomed.*, 2019, **14**, 205–214.
63 D. Sun, Z. Chen, M. Wu and Y. Zhang, *Nanotheranostics*, 2017, **1**, 389–402.
64 J. T. Dong, J. F. Chen, M. Smalley, M. P. Zhao, Z. F. Ke, Y. Z. Zhu and H. R. Tseng, *Adv. Mater.*, 2020, **32**, e1903663.
65 Z. Jahed, R. Zareian, Y. Y. Chau, B. B. Seo, M. West, T. Y. Tsui, W. J. Wen and M. R. K. Mofrad, *ACS Appl. Mater. Interfaces*, 2016, **8**, 23604–23613.
66 A. Cutarelli, S. Ghio, J. Zasso, A. Speccher, G. Scarduelli, M. Roccuzzo, M. Crivellari, N. M. Pugno, S. Casarosa, M. Boscardin and L. Conti, *Cells*, 2020, **9**, 88.
67 A. A. Chang, J. N. Patel, C. Cordoba, B. Kaminska and K. Kavanagh, *SPIE Conf. Proc.*, 2014, **8973**, 89730J.
68 K. Y. Hwang, J. H. Kim, K. Y. Suh, J. S. Ko and N. Huh, *Sens. Actuators, B*, 2011, **155**, 422–429.
69 P. T. Wang, J. W. Su, W. Dai, G. Cernigliaro and H. W. Sun, *Appl. Phys. Lett.*, 2014, **104**, 043504.
70 B. P. Zhou, W. Xu, A. A. Syed, Y. Y. Chau, L. Q. Chen, B. Chew, O. Yassine, X. X. Wu, Y. B. Gao, J. X. Zhang, X. Xiao, J. Kosel, X. X. Zhang, Z. H. Yao and W. J. Wen, *Lab Chip*, 2015, **15**, 2125–2132.
71 S. Krishnamoorthy, Z. Y. Zhang and C. X. Xu, *Bio-Des. Manuf.*, 2020, **3**, 60–70.
72 C. Alix-Panabieres and K. Pantel, *Lab Chip*, 2014, **14**, 57–62.
73 Y. T. Xiong, H. Y. Kang, H. Z. Zhou, L. Ma and X. B. Xu, *Bio-Des. Manuf.*, 2022, **5**, 607–616.
74 D. Y. Hu, H. Liu, Y. Tian, Z. Li and X. Y. Cui, *ACS Comb. Sci.*, 2020, **22**, 701–711.
75 S. Park, R. R. Ang, S. P. Duffy, J. Bazov, K. N. Chi, P. C. Black and H. S. Ma, *PLoS One*, 2014, **9**, e85264.
76 F. Guilak, J. R. Tedrow and R. Burgkart, *Biochem. Biophys. Res. Commun.*, 2000, **269**, 781–786.
77 L. R. Huang, E. C. Cox, R. H. Austin and J. C. Sturm, *Science*, 2004, **304**, 987–990.
78 P. T. Went, A. Lugli, S. Meier, M. Bundi, M. Mirlacher, G. Sauter and S. Dirnhofer, *Hum. Pathol.*, 2004, **35**, 122–128.
79 J. P. Gleghorn, E. D. Pratt, D. Denning, H. Liu, N. H. Bander, S. T. Tagawa, D. M. Nanus, P. A. Giannakakou and B. J. Kirby, *Lab Chip*, 2010, **10**, 27–29.
80 W. Y. Qian, Y. Zhang and W. Q. Chen, *Small*, 2015, **11**, 3850–3872.
81 E. J. Cho, J. W. Lee and A. D. Ellington, *Annu. Rev. Anal. Chem.*, 2009, **2**, 241–264.
82 H. T. Ma, J. P. Liu, M. M. Ali, M. A. I. Mahmood, L. Labanieh, M. R. Lu, S. M. Iqbal, Q. Zhang, W. A. Zhao and Y. Wan, *Chem. Soc. Rev.*, 2015, **44**, 1240–1256.
83 J. Cao, X. P. Zhao, M. R. Younis, Z. Q. Li, X. H. Xia and C. Wang, *Anal. Chem.*, 2017, **89**, 10957–10964.
84 L. K. Liu, K. G. Yang, H. Gao, X. Li, Y. B. Chen, L. H. Zhang, X. J. Peng and Y. K. Zhang, *Anal. Chem.*, 2019, **91**, 2591–2594.
85 M. Poudineh, M. Labib, S. Ahmed, L. N. M. Nguyen, L. Kermanshah, R. M. Mohamadi, E. H. Sargent and S. O. Kelley, *Angew. Chem., Int. Ed.*, 2017, **56**, 163–168.
86 Y. J. Zhao, D. K. Xu and W. H. Tan, *Integr. Biol.*, 2017, **9**, 188–205.
87 H. J. Yoon, M. Kozminsky and S. Nagrath, *ACS Nano*, 2014, **8**, 1995–2017.
88 J. X. Meng, P. C. Zhang, F. L. Zhang, H. L. Liu, J. B. Fan, X. L. Liu, G. Yang, L. Jiang and S. T. Wang, *ACS Nano*, 2015, **9**, 9284–9291.
89 H. Y. Yue, S. Huang, J. Chang, C. Heo, F. Yao, S. Adhikari, F. Gunes, L. C. Liu, T. H. Lee, E. S. Oh, B. Li, J. J. Zhang, T. Q. Huy, N. V. Luan and Y. H. Lee, *ACS Nano*, 2014, **8**, 1639–1646.
90 S. T. Wang, H. Wang, J. Jiao, K. J. Chen, G. E. Owens, K. I. Kamei, J. Sun, D. J. Sherman, C. P. Behrenbruch, H. Wu and H. R. Tseng, *Angew. Chem., Int. Ed.*, 2009, **48**, 8970–8973.
91 J. Sekine, S. C. Luo, S. Wang, B. Zhu, H. R. Tseng and H. Yu, *Adv. Mater.*, 2011, **23**, 4788–4792.
92 N. A. Zhang, Y. L. Deng, Q. D. Tai, B. R. Cheng, L. B. Zhao, Q. L. Shen, R. X. He, L. Y. Hong, W. Liu, S. S. Guo, K. Liu, H. R. Tseng, B. Xiong and X. Z. Zhao, *Adv. Mater.*, 2012, **24**, 2756–2760.
93 Y. T. Lu, L. B. Zhao, Q. L. Shen, M. A. Garcia, D. X. Wu, S. Hou, M. Song, X. C. Xu, W. H. OuYang, W. W. L. OuYang, J. Lichterman, Z. Luo, X. Xuan, J. T. Huang, L. W. K. Chung, M. Rettig, H. R. Tseng, C. Shao and E. M. Posadas, *Methods*, 2013, **64**, 144–152.
94 S. Hou, H. C. Zhao, L. B. Zhao, Q. L. Shen, K. S. Wei, D. Y. Suh, A. Nakao, M. A. Garcia, M. Song, T. Lee, B. Xiong, S. C. Luo, H. R. Tseng and H. H. Yu, *Adv. Mater.*, 2013, **25**, 1547–1551.
95 M. Lin, J. F. Chen, Y. T. Lu, Y. Zhang, J. Z. Song, S. Hou, Z. F. Ke and H. R. Tseng, *Acc. Chem. Res.*, 2014, **47**, 2941–2950.
96 S. Guo, J. Q. Xu, M. Xie, W. Huang, E. F. Yuan, Y. Liu, L. P. Fan, S. B. Cheng, S. M. Liu, F. B. Wang, B. F. Yuan, W. G. Dong, X. L. Zhang, W. H. Huang and X. Zhou, *ACS Appl. Mater. Interfaces*, 2016, **8**, 15917–15925.

97 F. L. Zhang, Y. Jiang, X. L. Liu, J. X. Meng, P. C. Zhang, H. L. Liu, G. Yang, G. N. Li, L. Jiang, L. J. Wan, J. S. Hu and S. T. Wang, *Nano Lett.*, 2016, **16**, 766–772.
98 L. Wang, S. Huang, Q. Y. Li, L. Y. Ma, C. Zhang, F. Liu, M. Jiang, X. Yu and L. Xu, *Chem. Eng. J.*, 2022, **435**, 134762.
99 J. J. Gu, W. Zhang, H. L. Su, T. X. Fan, S. M. Zhu, Q. L. Liu and D. Zhang, *Adv. Mater.*, 2015, **27**, 464–478.
100 H. Cui, Q. Liu, R. Li, X. Y. Wei, Y. Sun, Z. X. Wang, L. L. Zhang, X. Z. Zhao, B. Hua and S. S. Guo, *Nanoscale*, 2020, **12**, 1455–1463.
101 J. J. VanDersarl, A. M. Xu and N. A. Melosh, *Nano Lett.*, 2012, **12**, 3881–3886.
102 X. Xie, A. M. Xu, S. Leal-Ortiz, Y. H. Cao, C. C. Garner and N. A. Melosh, *ACS Nano*, 2013, **7**, 4351–4358.
103 Y. H. Cao, M. Hjort, H. D. Chen, F. Birey, S. A. Leal-Ortiz, C. M. Han, J. G. Santiago, S. P. Pasca, J. C. Wu and N. A. Melosh, *Proc. Natl. Acad. Sci. U. S. A.*, 2017, **114**, E1866–E1874.
104 A. M. Xu, S. A. Kim, D. S. Wang, A. Aalipour and N. A. Melosh, *Lab Chip*, 2016, **16**, 2434–2439.
105 W. L. Gao, H. J. Yuan, F. X. Jing, S. Wu, H. B. Zhou, H. J. Mao, Q. H. Jin, J. L. Zhao, H. Cong and C. P. Jia, *Oncotarget*, 2017, **8**, 12917–12928.
106 K. Yoneda, T. Kuwata, Y. Chikaishi, M. Mori, M. Kanayama, M. Takenaka, S. Oka, A. Hirai, N. Imanishi, K. Kuroda, Y. Ichiki, T. Ohnaga and F. Tanaka, *Cancer Sci.*, 2019, **110**, 726–733.
107 X. F. Zhang, X. Lu, W. L. Gao, Y. M. Wang, C. P. Jia and H. Cong, *Transl. Oncol.*, 2021, **14**.
108 V. Murlidhar, R. M. Reddy, S. Fouladdel, L. L. Zhao, M. K. Ishikawa, S. Grabauskiene, Z. Zhang, J. Lin, A. C. Chang, P. Carrott, W. R. Lynch, M. B. Orringer, C. Kumar-Sinha, N. Palanisamy, D. G. Beer, M. S. Wicha, N. Ramnath, E. Azizi and S. Nagrath, *Cancer Res.*, 2017, **77**, 5194–5206.
109 K. Kure, M. Hosoya, T. Ueyama, M. Fukaya, K. Sugimoto, Y. Tomiki, T. Ohnaga, K. Sakamoto and H. Komiyama, *Oncol. Lett.*, 2020, **19**, 2286–2294.
110 M. Kanayama, T. Kuwata, M. Mori, Y. Nemoto, N. Nishizawa, R. Oyama, H. Matsumiya, A. Taira, S. Shinohara, M. Takenaka, K. Yoneda, K. Kuroda, T. Ohnaga and F. Tanaka, *Cancer Sci.*, 2022, **113**, 1028–1037.
111 Y. Zhang, X. F. Zhang, J. L. Zhang, S. Sun, L. L. Zheng, J. Li, S. X. Liu, G. D. Sui and Z. F. Yin, *Cancer Biol. Ther.*, 2016, **17**, 1177–1187.
112 X. Yu, N. Wu, F. Chen, J. Wei and Y. X. Zhao, *Trends Anal. Chem.*, 2019, **117**, 27–38.
113 Y. Z. Zhu, D. Joralmon, W. T. Shan, Y. Y. Chen, J. H. Rong, H. Y. Zhao, S. Q. Xiao and X. J. Li, *Bio-Des. Manuf.*, 2021, **4**, 405–428.
114 V. Mehta and S. N. Rath, *Bio-Des. Manuf.*, 2021, **4**, 311–343.